

Application of Irreversible Thermodynamics to Distillation

Gelein M. de Koeijer *

Statoil ASA, Research & Technology, Corporate Strategic Technology
Arkitekt Ebbellsvei 10, 7005 Trondheim, Norway
Tel: +47 73584011, Fax: +47 73967286
E-mail: gdek@statoil.com

Signe Kjelstrup

Norwegian University of Science and Technology,
Department of Chemistry
Sem Sælandsvei 14, 7491 Trondheim, Norway

Abstract

We compare three different ways of modelling tray distillation to each other, and to experimental data: the most common way that assumes equilibrium between the liquid and vapour phases at the outlets of each tray, and two more precise methods that use irreversible thermodynamics. Irreversible thermodynamics determines the driving forces and fluxes of a system in agreement with the second law. It is shown that the methods using irreversible thermodynamics (Maxwell-Stefan equations) are superior to the method that assumes that equilibrium is reached on each tray. The Soret effect must be included to have a good description of the heat flux.

Keywords: Irreversible Thermodynamics, Distillation, Maxwell-Stefan Equation, Soret/Dufour effects, Interface.

1. Introduction

Distillation is the most common separation method: It accounts for 11 % of the industrial energy demand in the USA in 1991 (Humphrey and Siebert 1992). Since industrial scale experiments are demanding and expensive, distillation models are useful for design of distillation columns. Tray distillation is most commonly modelled by assuming that equilibrium is established between the vapour and the liquid at the outlets of each tray in the column. However, in reality equilibrium is not reached. The first attempt to account for the irreversible nature of the process was to introduce tray efficiencies. The Murphree efficiency measures to which degree equilibrium is reached (King 1980). The Murphree efficiency has been used to describe distillation with some success for binary mixtures at steady state. The method breaks down for multi-component systems or for dynamic behaviour. Moreover, the Murphree efficiency provides no physical explanation for why equilibrium is not reached.

Descriptions that introduce such explanations have their origin in irreversible thermodynamics (Kuiken 1994, Forland et al.

2001, Demirel and Sandler 2001). In irreversible thermodynamics the fluxes and forces of the system are derived in a systematic way: All possible coupling effects can be included, or discarded, within a framework that complies with the second law. The pioneering articles, in that irreversible thermodynamics was applied to distillation, were written by Krishnamurthy and Taylor (1985a, 1985b). These authors modelled distillation by means of driving forces and transfer rates without the assumption of equilibrium between the liquid and the vapor at the outlets of a tray. Interestingly, the authors did not expect the results to be that good at first try. The transfer rates were formulated using Maxwell-Stefan equations, and this approach is therefore called the Maxwell-Stefan approach from now on. Research using this approach is now described in books (Taylor and Krishna 1993, Perry and Green 1997, Seader and Henley 1998) and reviewed by Krishna and Wesselingh (1997). The increased computing capacity and speed has helped to develop the Maxwell-Stefan approach.

Instead of assuming equilibrium between the liquid and vapour at the outlets of each tray, in the Maxwell-Stefan approach one introduces a

*Author to whom correspondence should be addressed

liquid film and a vapour film with gradients in temperature and concentration. The films meet at the interface, where equilibrium is assumed between the vapour and liquid, however. Its development is now in direction of three-phase distillation (Eckert and Vanek, 2001), reactive distillation (Taylor and Krishna 2000), zeolites (Kapteijn et al. 2000) and membranes (Krishna and Wesselingh 1997). There are, however, questionable assumptions in this approach (Alopeaus and Aittamaa 2000, Olivier 2002, Kjelstrup and De Koeijer 2003).

The general development of non-equilibrium models may benefit from having also a more general formulation, through which the commonly used Maxwell-Stefan approach can be tested. One such formulation, called the interface integrated approach, was recently proposed by Kjelstrup and De Koeijer (2003), Bedeaux and Kjelstrup (2004). This approach introduces the complications of the Soret/Dufour effects and that there is no equilibrium over the interface. In Kjelstrup and De Koeijer (2003) the approach was related to the Maxwell-Stefan approach, but

not quantitatively compared with the available approaches and models. This work compares the performance of the Maxwell-Stefan approach, the interface integrated approach and the model assuming equilibrium reached on each tray for a binary tray distillation column that separates water and ethanol. Experimental data are used as a reference. The comparison is meant to give motivation for application of irreversible thermodynamics to distillation.

2. The System

In *Figure 1*, distillation is shown in three different scales. The whole column is drawn on the coarsest scale to the left. The tray is shown on the intermediate scale in the upper part of the figure, and the region around the liquid-vapour interface is shown below, on the smallest (10^{-3} - 10^{-5} m) scale. We focus on the smallest scale in this work. Heat and mass transfer in and out of the volume around the interface are considered. The system consists of a bulk vapour phase, a vapour film, an interface, a liquid film and a bulk liquid phase, all in series.

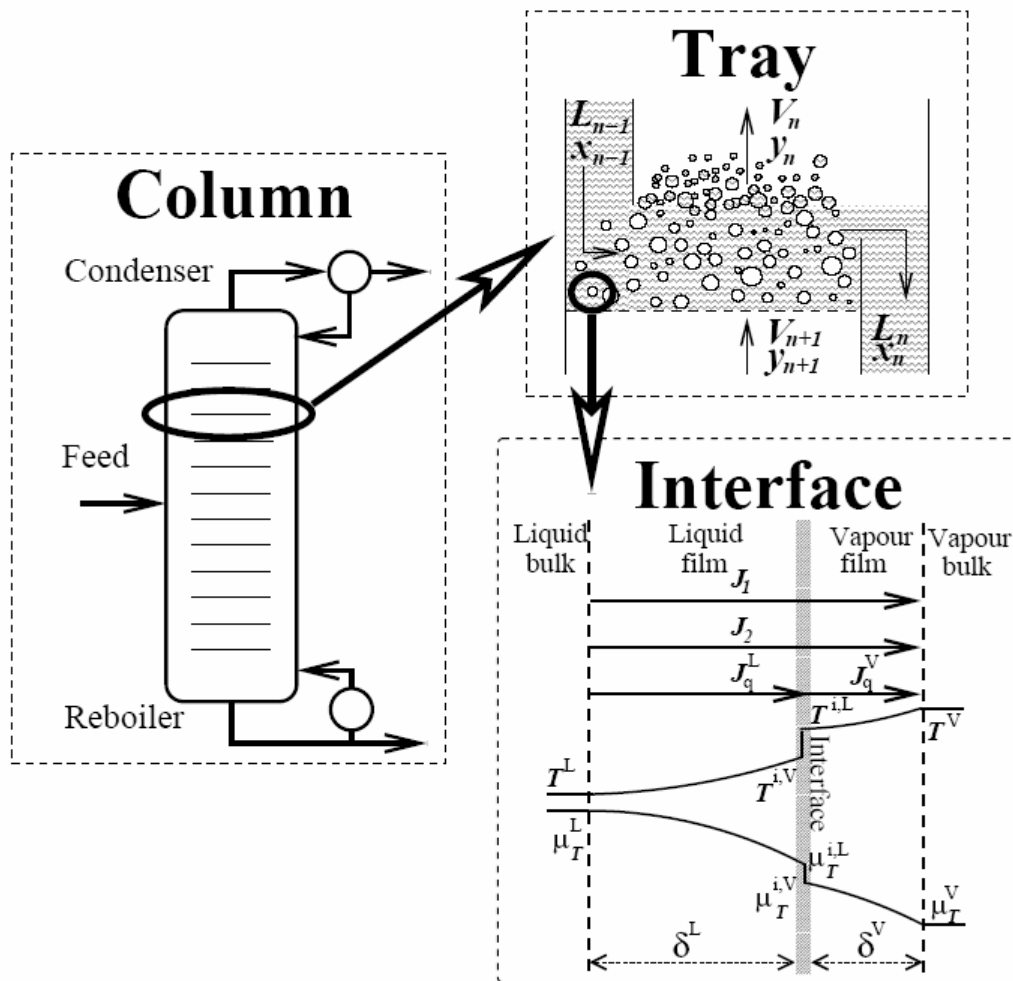


Figure 1. Three levels of system details: column, tray and interface. Symbols are described in the text.

We assume that the major part of the dissipation of energy takes place in the volumes of the vapour film, interface, and liquid film. The bulk phases are probably well mixed, and dissipation by turbulence is small. The Maxwell-Stefan and the interface integrated approaches deal with transport across this series of films in different ways.

3. The Entropy Production Rate

The rate equations are prescribed by the entropy production rate in irreversible thermodynamics. This ensures that the second law is fulfilled. The entropy production rate is given by the system's product sum of driving forces X and transfer rates. The transfer rate is the flux integrated over the transfer area. In distillation, one has the heat transfer rate, J_q^V in the vapour film, and the mass transfer rates, N_j for components j (in the interface frame of reference, see Taylor and Krishna (1993) for more information on frames of reference). The entropy production rate can be described by the constant mass transfer rates, the constant heat transfer rate in the vapour, and the respective average driving forces, X , (Kjelstrup and De Koeijer 2003):

$$\frac{dS^{irr}}{dt} = J_q^V X_q + \sum_{j=1}^J N_j X_j \quad (1)$$

The heat flux in the liquid (J_q^L in *Figure 1*) was eliminated using the energy balance. The driving forces are related to the transfer rates by resistances, r . For binary distillation, we have (Kjelstrup and De Koeijer 2003):

$$\begin{aligned} X_q &= \bar{r}_{qq} J_q^V + \bar{r}_{q1} N_1 + \bar{r}_{q2} N_2 \\ X_1 &= \bar{r}_{1q} J_q^V + \bar{r}_{11} N_1 + \bar{r}_{12} N_2 \\ X_2 &= \bar{r}_{2q} J_q^V + \bar{r}_{21} N_1 + \bar{r}_{22} N_2 \end{aligned} \quad (2)$$

Other relations are possible, but these are convenient, since in distillation the transfer rates are accurately available from experiments. All rate equations must comply with this scheme and use information on transport coefficients. The specific approaches that have been used so far are presented next.

3.1 The interface integrated approach

The interface integrated approach was derived and applied by Kjelstrup and De Koeijer (2003) and Bedeaux and Kjelstrup (2004). Kjelstrup and De Koeijer used the following average driving forces for heat and mass transfer:

$$\begin{aligned} X_{q,n} &= D_n \left(\frac{1}{T} \right) = \frac{1}{2} \left(\frac{1}{T_{n+1}} - \frac{1}{T_{n-1}} \right) \\ X_{j,n} &= \frac{D_n m_{j,T}}{T_n} = \end{aligned} \quad (3)$$

$$\frac{1}{2} \frac{R \ln \frac{x_{j,n-1} g_j(x_{j,n-1}) P_j^*(T_{n-1}) x_{j,n} g_j(x_{j,n}) P_j^*(T_n)}{y_{j,n} y_{j,n+1} P^2}}{y_{j,n} y_{j,n+1} P^2}$$

Transfer rates were given with the interface frame of reference:

$$N_{j,n} = V_n y_{j,n} - V_{n+1} y_{j,n+1} \quad (4)$$

The measurable heat transfer rate in the vapour film was derived from the energy balance over the vapour phase:

$$\begin{aligned} J_{q,n}^V &= (T_{n+1}^V - T_n^V) \frac{1}{2} (V_n [y_{1,n} C_{P,1}^V + y_{2,n} C_{P,2}^V] \\ &+ V_{n+1} [y_{1,n+1} C_{P,1}^V + y_{2,n+1} C_{P,2}^V]) \end{aligned} \quad (5)$$

Resistances were derived by integrating across the liquid film, the interface and the vapour film in *Figure 1*. The results were:

$$\begin{aligned} \bar{r}_{qq} &= \bar{r}_{qq}^{-i} + \bar{r}_{qq}^{-V} + \bar{r}_{qq}^{-L} \\ \bar{r}_{q1} &= \bar{r}_{1q}^{-i} = \bar{r}_{q1}^{-i} + \bar{r}_{q1}^{-V} + \bar{r}_{q1}^{-L} + \bar{r}_{qq}^{-L} D_{vap} H_1 \\ \bar{r}_{q2} &= \bar{r}_{2q}^{-i} = \bar{r}_{q2}^{-i} + \bar{r}_{q2}^{-V} + \bar{r}_{q2}^{-L} + \bar{r}_{qq}^{-L} D_{vap} H_2 \\ \bar{r}_{11} &= \bar{r}_{11}^{-i} + \bar{r}_{11}^{-V} + \bar{r}_{11}^{-L} + 2\bar{r}_{q1}^{-L} D_{vap} H_1 + \bar{r}_{qq}^{-L} D_{vap} H_1^2 \\ \bar{r}_{22} &= \bar{r}_{22}^{-i} + \bar{r}_{22}^{-V} + \bar{r}_{22}^{-L} + 2\bar{r}_{q2}^{-L} D_{vap} H_2 + \bar{r}_{qq}^{-L} D_{vap} H_2^2 \\ \bar{r}_{12} &= \bar{r}_{21}^{-i} = \bar{r}_{12}^{-i} + \bar{r}_{12}^{-V} + \bar{r}_{12}^{-L} + \bar{r}_{q1}^{-L} D_{vap} H_2 + \bar{r}_{q2}^{-L} D_{vap} H_1 \\ &+ \bar{r}_{qq}^{-L} D_{vap} H_1 D_{vap} H_2 \end{aligned} \quad (6)$$

These resistances are overall resistances for the series of layers, including the interface (superscripts i). There was no equilibrium across the interface. All resistances ($r_{jj}, r_{jq}, r_{qj}, r_{qq}$) for each film and interface were estimated from their respective resistivities:

$$\begin{aligned} \bar{r}^{-L} &= \frac{\delta^L}{A} r^L(T, x) & \bar{r}^{-V} &= \frac{\delta^V}{A} r^V(T, y) \\ \bar{r}^{-i} &= \frac{1}{A} r^i(T, y) \end{aligned} \quad (7)$$

They use the transfer area, A , and the film thicknesses, δ . The resistivities r^i of the interface can be taken from kinetic theory (Bedeaux et al. 1992, Kjelstrup and De Koeijer 2003), but this theory fails, when the mixture becomes non-ideal or is far away from the triple line (Olivier et al. 2002). The resistivities for the homogeneous phases were calculated from diffusion

coefficients, thermal conductivities and Soret coefficients, see Kjelstrup and De Koeijer (2003) for further details. As diffusion coefficients one uses Maxwell-Stefan diffusion coefficients (see below). The resistances \bar{r} depend on hydrodynamic variables like velocities, diameters, active tray area etc, via the film thickness and the area of transfer.

3.2 Maxwell-Stefan approach

The Maxwell-Stefan approach uses coupling between the diffusion of different components (Taylor and Krishna 1993):

$$-\nabla\mu_j = RT \sum_{k=1, k \neq j}^J \frac{x_k (u_j - u_k)}{D_{jk}} \quad (8)$$

In these equations u is the component velocity and D is the Maxwell-Stefan diffusion coefficient (which is different from the Fick's diffusion coefficient, see Kuiken (1994)). The equations can be used with any frame of reference, but normally the average molar velocity frame of reference is used in the further derivations. The heat-mass (Soret) coupling coefficients (\bar{r}_{jq} in equation (2)) are neglected (Taylor and Krishna 1993). This is often a good assumption in the bulk phases, but not at the interface (Røsforde et al. 2001). For distillation of a multi-component mixture, mass transfer rates J_j (in the molar average frame of reference) are derived from equation (8), and include diffusive and hydrodynamic contributions. In matrix equation notation, we have on tray n :

$$\begin{aligned} J_n^V &= c_{t,n}^V [k_n^V] (y_n^V - y_n^i)_{avg} \\ J_n^L &= c_{t,n}^L [k_n^L] (x_n^i - x_n^L)_{avg} \end{aligned} \quad (9)$$

The mass transfer rates depend on each other through:

$$\sum_{j=1}^J J_{j,n} = 0 \quad (10)$$

The heat transfer rate in each phase is given by the integrated heat flux. For the vapour phase:

$$J_{q,n}^V = h_n (T_n^V - T_n^L)_{avg} \quad (11)$$

All equations are integrated across the liquid and vapour films, using the equilibrium condition and the equation for energy conservation at the phase boundary.

The heat and mass transfer coefficients (h_n and the matrices $[k_n]$) are calculated using correlations that apply to the type of separator,

e.g. sieve tray column, bubble cap column, packed column etc. The correlations contain usually a product of dimensionless numbers, like the Reynolds, Sherwood, Prandtl, Schmidt and/or the Stanton numbers, and take into account that hydrodynamic conditions influence the extension of the films. In this manner, the transfer area (A) and the film thickness (δ) are included in the calculations indirectly. Most commonly, one finds either the heat transfer coefficient or the mass transfer coefficient, and calculates the other by the Chilton-Colburn analogy. Momentum conservation equations (i.e. pressure drop over the tray) can be added without increasing the complexity much.

The Maxwell-Stefan approach for distillation is used in commercially available software: ChemSep (2003) (developed by A. Haket, H. Kooijman, R. Taylor and H. Wesselingh) and the function RateFrac in the flowsheeter Aspen Plus (2003). The columns are modelled by simultaneously solving the mass and energy balances, equilibrium equations, and rate equations (see equation (9)) with given parameters on feed, distillate, bottom and tray design. For more details on the calculations see Taylor and Krishna (1993) and Seader and Henley (1998).

4. Calculations

As reference for the simulations we used the experimental data of a pilot-scale rectifying column from Rivero (1993) and De Koeijer and Rivero (2003). The column separated a water-ethanol feed of 0.331 mol/s with an ethanol mole fraction of 0.0710. The distillate had an ethanol mole fraction of 0.7073 and the bottom 0.0074. The experiments gave the mole fractions and the liquid temperatures on each tray. The entropy production rate and the transfer rates were calculated from these data using mass-, energy-, and entropy balances, see Rivero (1993). The same column was modelled using the above mentioned in- and outputs as boundary conditions, and the following methods:

1. The assumption of equilibrium between liquid and vapour outlets on each tray.
2. The Maxwell-Stefan equations (9) and (11).
3. The interface integrated approach using the resistances in Eq. (6).

The first method was a simulation with the flowsheeter ProVision (2003). Non-Random Two Liquid (NRTL) activity coefficients were used for the liquid mixtures. In the second method the column was simulated using ChemSep (2003) based on Taylor and Krishna (1993), with the DECHEMA model and NRTL

activity coefficients for the liquid. The Wilke-Chang equation for diffusion in the liquid was used. Design parameters for the sieve tray column were taken from De Koeijer and Rivero (2003), repeated in TABLE I. Other parameters in Provision and ChemSep were set to default.

TABLE I. DESIGN PARAMETERS OF COLUMN

Design Parameter	Value
Number of trays	10
Total column height [m]	2.90
Tray spacing [m]	0.275
Column diameter [cm]	15
Weir height [cm]	2.0
Total plate area [cm ²]	176.7
Active plate area [cm ²]	154.6
Hole diameter [mm]	2
Total hole area [cm ²]	23.2

For the third method the data set was taken from Kjelstrup and De Koeijer (2003) with a ratio of the liquid and vapour film thicknesses of 10, and a ratio of liquid film thickness and transfer area (δ^L/A) of $6.7 \cdot 10^{-4} \text{ m}^{-1}$. In methods 2 and 3, the vapour was modelled using the ideal gas law, and the vapour pressure by the Antoine equation.

Methods 1 and 2 were first used to find the mole fraction profile of the column. Method 3 used the experimental liquid mole fraction as input, since the method is not yet so fully developed that it provides a full solution of the equations. We next calculated the entropy production rate on all trays with all methods, using equation (1). This equation described the entropy production rate satisfactory for this particular column in De Koeijer and Rivero (2003).

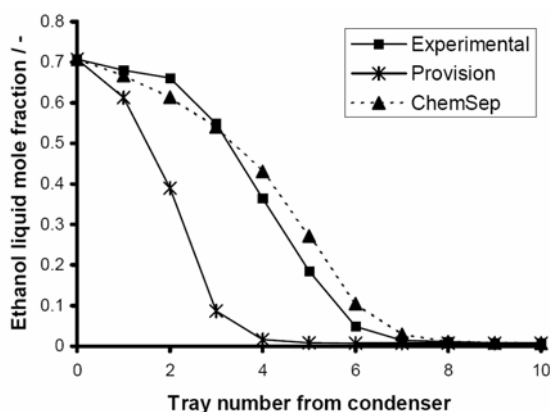


Figure 2. The ethanol liquid mole fraction of experimental data, ChemSep simulation and ProVision simulation

5. Results

The mole fraction profiles for ethanol, as predicted by the methods that provide a solution, ProVision and by ChemSep, are shown in Figure 2. The experimental data are also shown for comparison. The condenser duty was the common adjustable variable in the Provision and ChemSep simulations. They were respectively 1322 and 1343 Watt, while the experimental value was 1328 Watt.

Figure 3 shows the entropy production rate from the experimental data, the ChemSep simulation, the ProVision simulation, and from the interface integrated approach (using the experimental data).

6. Discussion

By inspection of Figure 2, one can conclude that the equilibrium model (1) fails to predict the experimental compositions. The Maxwell-Stefan approach (2) by means of ChemSep has a far better predictive power for compositions. Between tray numbers 0-3, the liquid mole fractions were max 0.05 units lower, and between trays 3-10 they were max 0.09 units higher than experimental values. These deviations are larger than the experimental error of 0.008 (Rivero 1993), however. The interface integrated approach (3) used the experimental mole fraction as input and can therefore not be discussed in a similar manner. The estimate for the condenser duty with ChemSep was close to the experimental value, while the one for the equilibrium simulation was nearly correct. So, a good condenser duty estimate does not necessarily mean a good estimate for the compositions.

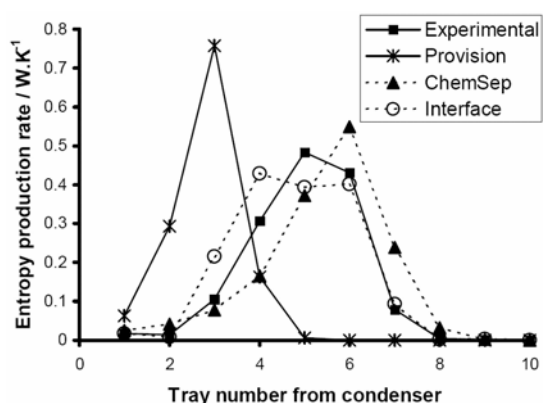


Figure 3. The entropy production rate (Eq.1) from experimental data, ChemSep simulation, ProVision simulation and interface-integrated approach

The differences in the mole fractions that are used in the three models, are reflected in the entropy production rate, see *Figure 3*. We see from this figure that the equilibrium model (1) fails to predict the magnitude as well as the location of the entropy production in the column. The non-equilibrium models, however, give both a fair prediction of both. The Maxwell-Stefan approach (2) predicts somewhat smaller values for trays 4-6, and higher values for trays 6 and 7. The interface integrated approach (3) was fitted to the entropy production with the ratio (δ^L/A) as variable. It gave the largest deviation from the experimental values in trays 3 to 5.

It is clear from *Figures 2* and *3* that, besides the condenser duty, the equilibrium model is inaccurate. Its only advantage is therefore its simplicity, and need for less information. In order to properly describe the entropy production in the column, irreversible thermodynamics is needed, and thus also information on diffusion coefficients, thermal conductivities, transfer area, viscosity, gas/liquid velocities, and design parameters of the column.

The two non-equilibrium approaches differ by their choice of assumptions. The Maxwell-Stefan approach includes ways to deal with hydrodynamic effects, while the interface integrated approach does not. The interface integrated approach takes the Soret/Dufour effect and dissipation in the interface into account, while the Maxwell-Stefan approach does not. These differences can explain partly the different behaviour in *Figure 3*. The interface resistance was not significant in the example that was studied here (Kjelstrup and De Koeijer 2003). But the Soret/Dufour effect was found significant (Kjelstrup and De Koeijer 2003 and Olivier 2002). It is thus necessary for a correct description of the heat transfer rate in the vapor phase and probably therefore also for a correct mass transfer rate. The Maxwell-Stefan approach is developed far enough for industrial use by means of ChemSep (2003) and the RateFrac function in Aspen Plus (2003).

7. Conclusions

We have seen above that the most common equilibrium model does not give accurate information on binary tray distillation of ethanol and water, and that irreversible thermodynamics is needed for this. Application of irreversible thermodynamics to distillation dates back to 1985. It is well developed by means of the Maxwell-Stefan approach. With the interface integrated approach one is also able to avoid the assumption of equilibrium at the gas-liquid contact. Both approaches give physicochemical insight into the processes.

Further developments of the non-equilibrium models require knowledge of larger number of individual terms in Equations (2) and (9). Taylor and Krishna (1993) list several relations for mass- and heat transfer coefficients, and this list should be continued. Measurements of the temperature in the vapour phase can probably be used to reveal Soret / Dufour effects contributions, and give better predictions of the thermodynamic forces and the heat transfer rates in the column. Such measurements are lacking in the literature.

Non-equilibrium models are required to study dynamic distillation. Such approaches are also beneficiary for steady state modelling (Taylor and Krishna 1993). Packed columns, separation of strongly non-ideal mixtures (e.g. azeotropes), separation with trace components and columns with complex design are examples of separations for which non-equilibrium models most clearly outperform the equilibrium ones.

Non-equilibrium models should be used to model diabatic distillation (De Koeijer and Rivero 2003, Rivero 2001) and to perform second law optimisations (Røsjorde and Kjelstrup 2004). Such studies have so far mostly been done using equilibrium models. With more realistic models, also these studies will become more realistic.

Acknowledgements

Statoil ASA is thanked for giving Gelein de Koeijer the possibility to write this article. Discussions with Audun Røsjorde are appreciated.

Nomenclature

A	Transfer area [m ²]
c	Concentration [mol/m ³]
C _p	Heat capacity [J/mol K]
Δ _{vap} H	Heat of vaporisation [J/mol]
Đ	Maxwell-Stefan diffusion coefficient [m ² /s]
dS ^{irr} /dt	Entropy production rate [J/s K]
h	Heat transfer coefficient [J/K s]
J	Mass transfer rate in molar average velocity frame of reference [mol/s]
J _q	Measurable heat transfer rate [J/s]
L	Liquid flow [mol/s]
N	Mass transfer rate in interface frame of reference [mol/s]
P	Pressure [Pa]
R	Gas constant [J/mol K]
\bar{r}_{jj}	Mass-mass resistance [s J/mol ² K]
\bar{r}_{jq}	Mass-heat resistance [s/mol K]
\bar{r}_{qq}	Heat-heat resistance [s /K J]
r	Resistivity [various]

T	Temperature [K]
u	Velocity [m/s]
V	Vapour flow [mol/s]
X	Average driving force [J/mol K or 1/K]
x	Liquid mole fraction [-]
y	Vapour mole fraction [-]

Greek Letters

γ	Activity coefficient [-]
δ	Film thickness [m]
κ	Mass transfer coefficient [m ³ /s]
μ	Chemical potential [J/mol]

List of Super- and Subscripts

avg	Average
i	Interface
j,k	Component number
J	Number of components
L	Liquid
n	Tray number
q	Heat
T	At constant temperature
V	Vapour, Saturation

References

- Alopeaus, V., Aittamaa J., 2000, "Appropriate simplifications in calculation of mass transfer in a multicomponent rate-based distillation tray model", *Ind. Eng. Chem. Res.*, Vol. 39, No. 11, pp.4336–4345.
- Aspen plus, 2003, website, <http://www.aspentech.com> (accessed January 2003).
- ChemSep. Website, 2003. website, <http://www.chemsep.org> (accessed January 2003).
- Bedeaux, D. and Kjelstrup, S., 2004, "Irreversible thermodynamics – a tool to describe phase transitions far from global equilibrium", *Chem. Eng. Sc.*, Vol.59, pp.109–118
- Bedeaux D., Smit, J.A.M, Hermans, L.F.J., Ytrehus, T., 1992, "Slow evaporation and condensation. 2. A dilute mixture", *Physica A*, Vol. 182, pp.388–418.
- De Groot, S.R., Mazur, P., 1984, *Non-Equilibrium Thermodynamics*, Dover, London.
- De Koeijer, G.M., Rivero, R., 2003, "Entropy production and exergy loss in experimental distillation columns", *Chem. Eng. Sc.*, Vol. 58, No. 8, pp.1587–1597.
- Demirel, Y., Sandler, S.I., 2001, "Linear nonequilibrium thermodynamics for coupled heat and mass transport", *Int. J. of Heat and Mass Transfer*, Vol. 44, pp.2439–2451.
- Eckert, E., Vanek, T, 2001, "Some aspects of rate-based modelling and simulation of three phase distillation columns", *Comp. Chem. Eng.*, Vol. 25, pp.603–612.
- Forland, K.S., Førland, T., Kjelstrup, S., 2001, *Irreversible Thermodynamics. Theory and Application*, Tapir, Trondheim, Norway, 3rd edition.
- Humphrey, J.L., Siebert, A.F., 1992, "Separation technologies: An opportunity for energy savings", *Chem. Eng. Progr.*, Vol. 88, No. 3, pp.32–41.
- Kapteijn, F., Moulijn, J.A., Krishna, R., 2000, "The generalized Maxwell-Stefan model for diffusion in zeolites: sorbate molecules with different saturation loadings", *Chem. Eng. Sc.*, Vol.55, No.15, pp.2923–2930.
- King, C.J., 1980, *Separation Processes*, McGraw-Hill, New York, 2nd edition.
- Kjelstrup, S., De Koeijer, G.M., 2003, "Transport equations for distillation of ethanol and water from the entropy production rate", *Chem. Eng. Sci.*, Vol.58, No.7, pp.1147–1161.
- Krishna, R., Wesselingh, J.A., 1997, "The Maxwell-Stefan approach to mass transfer", *Chem. Eng. Sc.*, Vol. 52, No.6, pp.861–911.
- Krishnamurthy, R., Taylor, R., 1985a, "A nonequilibrium stage model of multicomponent separation processes. Part I: Model description and method of solution", *AIChE Journal*, Vol.31, pp.449–456.
- Krishnamurthy, R., Taylor R., 1985b, "A nonequilibrium stage model of multicomponent separation processes. Part II: Comparison with experiment", *AIChE Journal*, Vol.31, pp.456–465.
- Kuiken, G.D.C., 1994, *Thermodynamics of Irreversible Processes*, John Wiley and Sons, Chichester, England.
- Olivier, M.L., 2002, "Development of a nonequilibrium mass and heat transfer computation in multiphase hydrocarbon system", PhD thesis, Norwegian University of Science and Technology, Department of Refrigeration and Air Conditioning, Trondheim, Norway, ISBN 82-471-5527-3, ISSN 0809-103X.
- Olivier, M.L., Rollier, J.D., Kjelstrup, S., 2002, "Equilibrium properties and surface transfer coefficients from molecular dynamics simulations of two-component fluids", *Colloids and Surfaces A: Physicochem. Eng. Aspects*, Vol. 210, pp.199–222.
- Y, R.H., Green, D.W., 1997, *Perry's Chemical Engineers Handbook*, McGraw-Hill, New York, 7th edition.
- Rivero, R., 1993, "L'Analyse d'Exergie: Application à la Distillation Diabatique et aux Pompes à Chaleur à Absorption", PhD thesis, Institut National Polytechnique de Lorraine, Nancy, France.

Rivero, R., 2001, "Exergy simulation and optimization of adiabatic and diabatic binary distillation", *Energy*, Vol.26, pp.561–593.

Røsjorde, A., Kjelstrup, S., Bedeaux, D., Hafskjold, B., 2001, "Nonequilibrium molecular simulations of steady-state heat and mass transport in condensation. II. Transfer coefficients", *Journal of Colloid Interface Science*, Vol.240, pp.355–364.

Røsjorde, A., Kjelstrup, S., 2004, "Second law optimisation of heat exchange area in diabatic binary tray distillation", Submitted.

Seader, J.D., Henley, E.J., 1998, *Separation process principles*, Wiley, New York.

SimSci, 2003, Provision, Website, <http://www.simsci.com> (accessed January 2003).

Taylor, R., Krishna, R., 1993, *Multicomponent Mass Transfer*, Wiley, New York.

Taylor, R., Krishna R., 2000, "Modelling reactive distillation", *Chem. Eng. Sc.*, Vol.55, pp.5183–5229.

Wesselingh, J.A., "Non-equilibrium modeling of distillation", *Chem. Engng. Research and Design (Trans. IChemE)*, Vol.75(A), pp.529–538.